Chapter 2

Generation of White Light Supercontinuum

Supercontinuum generation (SCG) is a process, where laser pulses with narrow spectral bandwidth (quasi-monochromatic) are converted to pulses with very broad spectral bandwidth.

If a high-peak-intensity pulse is focused into a transparent nonlinear material, the output pulse will, on a screen, appear as a white light flash, regardless of whether the input pulse is in the near IR or near UV range. The spectral broadening is mainly driven by the nonlinear optical effects of self-phase modulation (SPM), which leads to the generation of the new frequencies, and self-focusing (SF), which is responsible for very high peak intensities.

This phenomenon was first discovered with ps pulses by R. Alfano & S. Shapiro [ASh70] and remains an active field of research with applications for example in time-resolved spectroscopy [Ekv00], coherence tomography [HLC$^+$01], optical parametric amplification (OPA) [WYa97].

Continuum Generation in Sapphire

In this work the material used for SCG is an Al_2O_3 crystal often referred to as corundum or sapphire. It is known to afford a broadband SC and possesses a high damage threshold. Al_2O_3 is a centrosymmetric medium (i.e. it possess a center of inversion) that furthermore has no intrinsic free carriers, is non-conductive and non-magnetizable. These properties are essential to the SF and SPM effects involved in the CG.

2.1 Nonlinear Optical Effects

The interaction between an electromagnetic (EM) wave and the crystal, strongly depends on the strength of the electric field $\vec{E}(\vec{r},t)$.

If the amplitude $|\vec{E}(\vec{r},t)|$ of the electric field is much less than the inner Coulomb field of an atom (typically in the order of 10^9 V/m), the displacement of the electrons is small and the restoring force can follow electric-field linearly (harmonic oscillator). Thereby, the induced electric dipole moments are proportional to $\vec{E}(\vec{r},t)$, hence, the response is linear and results in a polarization $\vec{P}(\vec{r},t)$ of the medium, which is described by:

$$\vec{P}(\vec{r},t) = \varepsilon_0 \, \underline{\chi}^{(1)} \, \vec{E}(\vec{r},t) \; . \tag{2.1}$$

The proportionality factor $\underline{\chi}^{(1)}(\omega)$ is a 2nd-rank tensor and known as the linear susceptibility of the medium. It depends on the frequency of the incident EM field. In this chapter an instantaneous response of the medium without a reaction time, is assumed [Boy03]. In an isotropic material $\chi^{(1)}$ is a scalar quantity and related to the refractive index n of the material:

S. Uhlig, *Self-Organized Surface Structures with Ultrafast White-Light,* BestMasters,
DOI 10.1007/978-3-658-09894-0_2, © Springer Fachmedien Wiesbaden 2015

$$n = \sqrt{1 + \chi^{(1)}} \ . \tag{2.2}$$

If $|\vec{E}(\vec{r},t)|$ gets closer to the Coulomb field, the induced electric dipoles in the medium cannot respond linear anymore resulting from the anharmonic potential between the electrons and the nucleus, thus, higher order terms contribute to the polarization:

$$\vec{P}(\vec{r},t) = \vec{P}^{(1)} + \vec{P}^{(2)} + \vec{P}^{(3)} + ... = \varepsilon_0 \left[\underline{\chi}^{(1)} \ \vec{E} + \underline{\chi}^{(2)} \ \vec{E}\vec{E} + \underline{\chi}^{(3)} \ \vec{E}\vec{E}\vec{E} + ... \right] \ . \tag{2.3}$$

For sapphire with a centrosymmetric crystal structure, the even order susceptibility terms in Eq.(2.3) vanish [Boy03], so that only odd-order terms contribute to the polarization and cause distinct nonlinear effects.

2.1.1 Self-Focusing

The third-order nonlinear polarization is responsible for various phenomena. It can be related to processes like four-photon interactions (third harmonic generation, THG, and four wave-mixing), or nonlinear response effects of the material. One of the most important effects is the nonlinear contribution to the refractive index, which gives rise to various self-action effects of the laser beam like self-focusing in a crystal.

Higher-orders of nonlinearity can be neglected, since their strength of susceptibility decreases $\chi^{(n)}/\chi^{(n+1)} \approx 10^{12}$ [Boy03]. For demonstration it's easier to further assume a linearly polarized field in a dispersionless, isotropic medium. Then, the tensor character of $\underline{\chi}^{(3)}$ and the vector notation can be suppressed, leading to the medium total third-order response of:

$$P = P^{(1)} + P^{(3)} = \varepsilon_0 \left[\chi^{(1)} + \frac{3}{4} \chi^{(3)} \left| E(\omega) \right|^2 \right] E(\omega) \ . \tag{2.4}$$

The factor of 3/4 rises from the summation over all permutations of the four photon interaction, as well as the assumed simplifications [Boy03]. The expression in the brackets is also referred to as the effective susceptibility $\chi_{eff} = \chi_L + \chi_{NL}$, containing a linear and nonlinear term. Hence, a nonlinear contribution is added to the material's refractive index in Eq.(2.2):

$$n^2 = 1 + \chi_L + \chi_{NL} = n_0^2 + \frac{3}{4} \chi^{(3)} \left| E(\omega) \right|^2 \ . \tag{2.5}$$

Equation (2.5) can be rewritten and it can be shown that the nonlinear contribution is significantly less than the linear one and the following estimation can be applied.

$$n = n_0 \cdot \sqrt{1 + \frac{\chi_{NL}}{n_0^2}} \overset{\chi_{NL} \ll n_0^2}{\approx} n_0 \cdot \left(1 + \frac{1}{2} \frac{\chi_{NL}}{n_0^2} \right) \tag{2.6}$$

With the intensity $I = \frac{1}{2} \varepsilon_0 c n_0 \left| E \right|^2$ the nonlinear susceptibility becomes $\chi_{NL} = \frac{3}{2} \frac{\chi^{(3)} I}{\varepsilon_0 c n_0}$. Hence, the total refractive index is finally expressed as:

$$n \approx n_0 + \frac{3}{4} \frac{\chi^{(3)}}{\varepsilon_0 c n_0^2} I =: n_0 + n_2 I \ . \tag{2.7}$$

The quantity $n_2 = \frac{3}{4}\frac{\chi^{(3)}}{\varepsilon_0 c n_0^2}$ is the induced nonlinear refractive index. In Al_2O_3, the refractive index has a value of n_0=1.76 (@800nm) and its nonlinear contribution n_2=2.9×10^{-16}cm^2/W [Boy03]. Thus, a laser with an intensity of 1TW/cm^{-2} can produce a refractive index change of 2.9×10^{-4} in Al_2O_3. Now, this may seem not much, but can have a significant effect.

For a Gaussian laser beam, the spatial intensity profile results in a spatial variation of refraction index, which is higher in the center than at the wings. This variation in refraction index acts as a positive lens (self-focusing) and the beam converges and eventually collapses in one point.

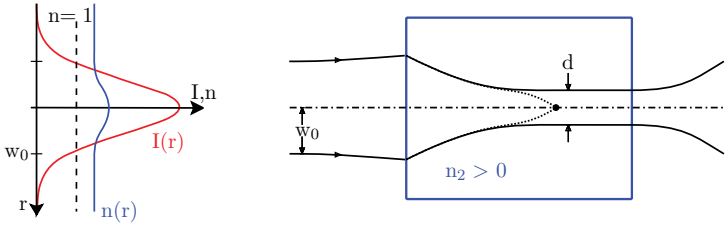

Figure 2.1: *r. Schematics of the intensity profile of a real laser beam and the corresponding refraction index. l. Beam diameter and self-focusing effect in a nonlinear optical medium.*

The occurrence of self-focusing, surprisingly, depends on the beam's power, rather than its intensity, and takes place only if a critical power is reached. In the theory of SF, J.H. Marburger [Mar75] calculated a threshold power for a Gaussian continuous wave (CW) laser beam with a wavelength λ_{laser}:

$$P_{crit} = \frac{3.77\lambda_{laser}^2}{8\pi n_0 n_2} \; . \tag{2.8}$$

For a CW-laser with λ_{laser}=800nm in Al_2O_3, this would equal a critical power of $P_{crit} \approx$ 1.88MW. However, for an ultra-short pulse duration, it has been reported that this threshold is considerably increased due to a temporal spread of the pulse (group velocity dispersion (GVD)) in a dispersive medium such as Al_2O_3 [CPe92], [SCo94], [LWM$^+$94].

If the applied power equals the critical power, another self-action effect, the so called *self-trapping* of light, occurs. Here, a defocusing balances the SF, preventing the beam from collapsing in one point and thus damaging the material. In this case, the beam acts as its own waveguide, propagating with a finite diameter d through the medium. It is reported that the beam in sapphire shrinks to a diameter of 20-25μm [BCh99], [YLW00], [JSM$^+$05].

The main cause of self-trapping and, thus, a limitation of self-focusing, is the generation of free electrons inside the medium [BCh99]. Thereby, a negative change in the index of refraction is induced, through the free-electron density N_e:

$$\Delta n_e = -\frac{2\pi e^2 N_e}{n_0 m_e \omega_{laser}^2}, \tag{2.9}$$

where ω_{laser} is the laser frequency. The main mechanism of free-electron generation in Al_2O_3, with femtosecond laser pulses, is multi-photon excitation (MPE).

Only in the central part of a Gaussian pulse (both spatial and temporal), where the intensity exceeds 10^{12} $[Wcm^{-2}]$, free-electrons can be generated in sapphire, through four-photon absorption. If the free-electron density reaches 10^{17}-10^{18} $[cm^{-2}]$ [JSM+05], [BCh99], Δn_e cancels out the nonlinear refraction index $n_2 I$ and self-focusing and defocusing come to an equilibrium. The lower intensity wings of the pulse are defocused due to diffraction.

For a pulse, which greatly exceeds the critical power P_{crit} for SF, the trapped beam, in transverse direction, breaks up in many separate beams (filaments), each of which contains the power P_{crit} and undergoes their own self-trapping effect. This is called *laser beam filamentation*. A Gaussian input beam becomes randomly modulated in intensity, overall reflecting the initial envelope with spots of higher intensity in the center. These spots, also referred to as *hotspots*, fluctuate over time in intensity, but in average keep their transverse position.

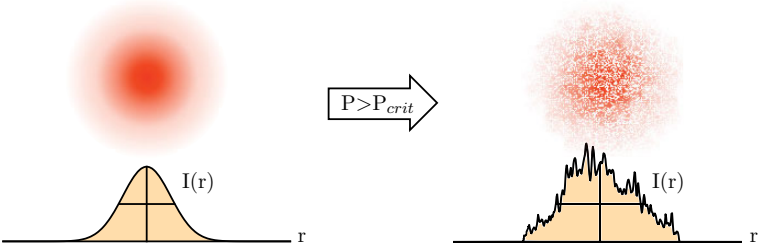

Figure 2.2: *Schematics of a Gaussian intensity distribution before (left) and after laser beam filamentation (right) as well as the corresponding transverse intensity profile. The beam breaks up in a large number of individual components each of which carries the power P_{crit}. p.a.m.f [Wik14].*

The nonlinear self-action effects of self-focusing, self-trapping and multi-beam filamentation are essential for the generation and enhancement of white-light supercontinuum. It is widely accepted that self-focusing triggers self-phase modulation.

2.1.2 Self-Phase Modulation

Self-phase modulation (SPM) is the dominant process for the generation of new frequencies from a fundamental laser frequency ω_0 in a nonlinear optical (NLO) medium such as sapphire. The mathematical description for the simple theory of SPM [YSh84], [Alf06] is straight forward and can be demonstrated as follows. The electric field of an incident laser pulse propagating in z direction can be expressed as,

$$E_{in}(z_0,t) = E_0(z,t)\ \mathrm{e}^{i(knz-\omega_0 t)}\ +\ c.c. = E_0(z,t)\ \mathrm{e}^{i\phi_0}\ +\ c.c. \tag{2.10}$$

where $k = \lambda/2\pi$ is the wave-number and n the material's refractive index. For simplicity, only the forward traveling wave is considered. Upon entering the NLO-medium of length L, the phase experiences an intensity dependent shift, in its propagation from 0 to L.

$$E_{out}(L,t) = E_0(L,t)\ \mathrm{e}^{i(kn_0L+kn_2I(t)L-\omega_0 t)} =: E_0(L,t)\ \mathrm{e}^{i(\phi_{NL}(L,t)+\phi_0)} \tag{2.11}$$

Note the time-dependence of the additional phase $\phi_{NL}(L,t)$, coming from the time-dependent intensity $I(t)$. The induced phase change $\Delta\phi = \phi_{NL} - \phi_0$, therefore, arises only from the intensity dependent refractive index of the material (Eq. 2.7). Since the frequency of the pulse's electric field is given by $\omega = -\left[\partial\left(\phi_{NL} + \phi_0\right)/\partial t\right]$, the phase modulation leads to a frequency modulation, with $k = \omega_0/c$,

$$\omega = \omega_0 - n_2 \frac{\omega_0}{c} L \frac{\partial I(t)}{\partial t} \ . \tag{2.12}$$

This situation is displayed in Fig. (2.3) for a τ_p=100fs pulse of a Gaussian intensity profile, with a peak intensity of 100TW/cm^2 in the temporal domain, that undergoes a frequency shift in a 5mm long Al_2O_3 crystal. The leading edge (the left-hand wing) is thereby shifted to lower

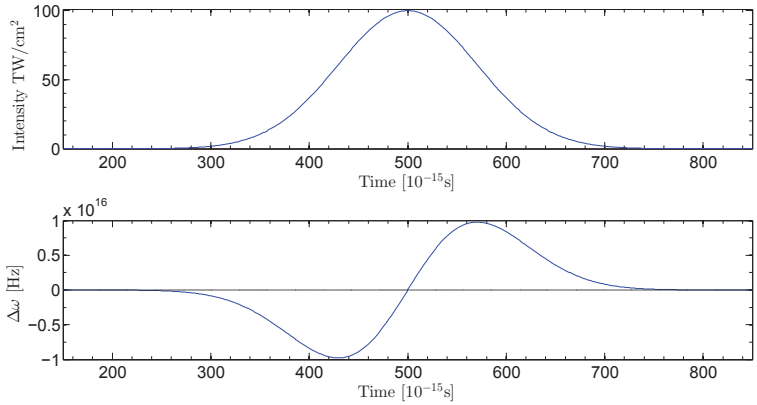

Figure 2.3: *(upper) temporal intensity profile a τ_p=100fs Gaussian laser pulse, (lower) frequency shift of the fundamental frequency ω_0 in a NLO-medium*

frequencies (i.e. longer wavelengths), whereas the trailing edge experiences a shift to higher frequencies (i.e. shorter wavelengths). The consequence is a broadening of the pulse spectrum $S(\omega)$ resulting from the time-dependent intensity slope, which can be calculated from the Fourier transformation. The corresponding spectrum of the output pulse is displayed in Fig.(2.4):

$$S(\omega) = |E_{out}(t)|^2 = \left| \int_{-\infty}^{\infty} E_0(t)\ \mathrm{e}^{-i\omega_0 t - i\phi_{NL}(z,t)}\ e^{i\omega t} \mathrm{dt} \right|^2 \ . \tag{2.13}$$

It shows a frequency broadening of about 2×10^{16}Hz in comparison to the fundamental laser frequency. Thus, the spectrum of the pulse spreads now from about 600nm up to 1000nm. The quasi-periodic oscillations of the spectrum, arise from symmetric phase change $\Delta\phi$, which further results from the symmetric intensity profile. Two newly generated waves (ω_1 & ω_2) with equal frequencies but different phases, can interfere constructively for $\Delta\phi_{12} = 2\pi$ or destructively for $\Delta\phi_{12} = \pi$. This example serves as a qualitative picture for demonstration of the SPM process.

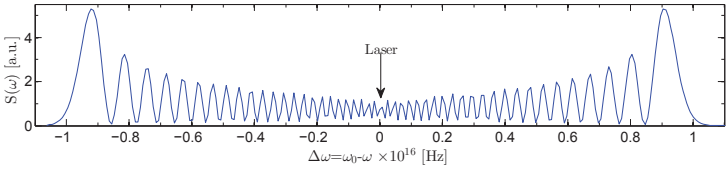

Figure 2.4: *Theoretical power spectrum of the phase modulated pulse with Gaussian temporal intensity distribution, which assumes an instantaneous response of the material.*

The red-shifted part of the spectrum is often referred to as Stokes broadening, while the blue-shifted part is referred to as anti-Stokes broadening. The displayed spectrum has a Stokes-anti-Stokes symmetry. Another consequence of the SPM is that the frequency of the output pulse changes over time, which means the pulse exhibits a high linear chirp.

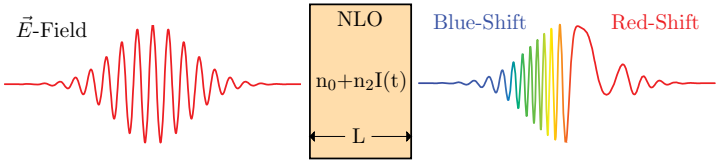

Figure 2.5: *SPM of a pulse (left) in a NLO-medium, results in a linear chirped output pulse (right).*

In this example of SPM an instantaneous response of the medium and, therefore, of n_2 was assumed. So, the phase modulation $\Delta\phi$ is directly proportional to the intensity variation $I(t)$. Generally, this is not the case. The medium's finite response time causes a distortion of the phase modulation $\Delta\phi$, which can result in a Stokes-anti-Stokes asymmetry, even if $I(t)$ is symmetric. Most spectra observed exhibit a strong anti-Stokes broadening (blue-shifted frequencies). This can qualitatively be explained as follows. The intensity dependence of the phase velocity $-\partial\phi[I(t)]/\partial t$ is responsible for the SPM, however, the intensity dependence of the group velocity (Eq.(2.14)) leads to the *self-steepening* of the pulse.

$$v_{\text{group}} = \frac{c}{n(I) + \omega \frac{\partial n(I)}{\partial \omega}} \tag{2.14}$$

From Equation (2.14) it follows, that the peak intensity of the pulse will have a smaller group velocity than its wings, because of the inverse proportionality to $I(t)$. Thus, the peak of the pulse falls away from the leading edge into the trailing edge, resulting in a steep intensity edge towards the back of the pulse. This higher slope in intensity will result in more blue-shifted frequencies towards the back of the pulse, than red-shifted and thus, in an asymmetric spectrum.

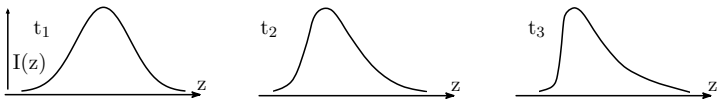

Figure 2.6: *Self-steepening of an incident Gaussian pulse with $t_1 < t_2 < t_3$. Typically the trailing edge exhibits a steepening, upon propagation through a NLO-Medium.*

Self-steepening, therefore changes the shape of the pulse. Self-phase modulation can also be considered in the spatial domain. In that case, the transverse intensity variations of the pulse lead to a nonlinear contribution to the refractive index $n_2 I(r)$ in transverse direction. Thus, the induced phase change $\Delta\phi(r, z)$ will cause a distortion of the wavefront and upon self-focusing, a drastic modification in the beam cross-section. As a consequence, different frequency components of the beam diffract into cones under different angles. If projected onto a screen, the continuum appears as a round white disk often surrounded by a distinct concentric rainbow-like pattern, also called *conical emission*, which exhibits a large divergence angle.

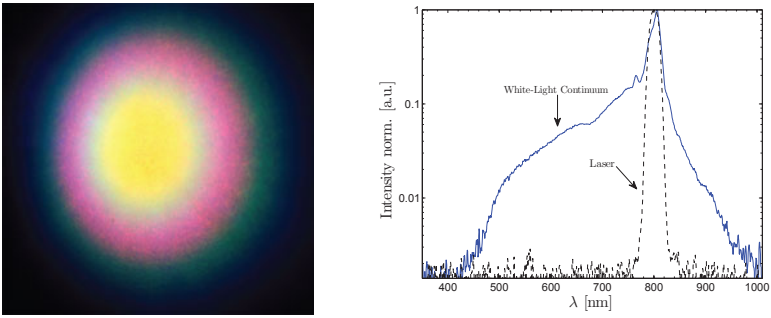

Figure 2.7: *White-light continuum from pump-laser (τ_p=75fs, λ=800nm) with a Gaussian intensity profile in Al_2O_3, projected onto a screen. Visible is white-light central disk and conical emission*

Diffraction is one explanation of the conical emission, but it has also been suggested that the effect could arise from four wave-mixing [XYA93], since the high divergence would satisfy the phase-matching condition. In Fig. (2.7) the output of a SC generated with femtosecond pulses (τ_p=75fs & λ=800nm), with a peak power of P_{peak}=1.56 GW per pulse, in Al_2O_3 is shown. The antisymmetric spectrum, taken in the center of the white-light disk, spreads from 450nm to 1000nm. It clearly shows a strong anti-Stokes broadening with more blue-shifted frequencies. The peak intensity of the WLC has about a tenth the intensity of the pump-laser.

The process of continuum generation only starts if a certain threshold is reached. Experimentally, it has been found that this threshold power equals the critical power for SF [TIm09], [BCh99]. However, during the SPM the new frequency components suffer a temporal lack due to group velocity dispersion in the medium. The pulse inevitably becomes longer and thus its peak intensity reduces, so that a higher input power is needed for SF to start. How much the pulse temporally spreads depends on the frequency components. In [QWW$^+$01] laser pulses (τ=130fs & λ=800nm) generated a WLC in H_2O, which spread from about 400nm to 1000nm. The individual frequency components showed an average WL pulse duration of 137fs. The WL pulse thereby propagated 1cm though the H_2O.

This shows that the WLC pulse stays an ultrafast light pulse during its generation and subsequent propagation in the NLO-medium. It thereby remains attractive for many physical applications that require ultrafast laser pulses such as femtosecond laser ablation.

http://www.springer.com/978-3-658-09893-3

Self-Organized Surface Structures with Ultrafast White-Light
First Investigation of LIPSS with Supercontinuum
Uhlig, S.
2015, IX, 97 p. 90 illus., Softcover
ISBN: 978-3-658-09893-3